



Permeable concrete mixed with various admixtures



Yail J. Kim ^{a,*}, Adel Gaddafi ^a, Isamu Yoshitake ^b

^a Department of Civil Engineering, University of Colorado Denver, Denver, CO 80217, United States

^b Department of Civil and Environmental Engineering, Yamaguchi University, Ube, Yamaguchi, Japan

ARTICLE INFO

Article history:

Received 23 October 2015

Received in revised form 29 February 2016

Accepted 19 March 2016

Available online 23 March 2016

Keywords:

Deterioration

Fiber

Fly ash

Infiltration

Live load

Multi-material interaction

Permeable concrete

ABSTRACT

This paper presents the performance of permeable concrete mixed with various alternative construction materials such as fly ash, fibers, and tire chips subjected to instantaneous live load intensity representing traffic-induced distress. Attention is paid to load-bearing capacity and hydraulic characteristics that affect the functionality of these concrete mixtures. Two test categories are examined depending upon the presence of fly ash and each category encompasses seven specimens with a combination of the admixture materials. Experimental results show that the inclusion of fly ash and tire chips decreases the load-carrying capacity of the permeable concrete, whereas that of fibers increases the capacity. The infiltration rate of the concrete is improved by the fibers and the degree of improvement is reliant upon their geometric configurations. Tire chips tend to clog pores and decreases infiltration. The instantaneous load intensity causes significant degradation in hydraulic conductivity, Reynolds number, and infiltration rate; particularly critical when mixed with fly ash. Predictive approaches based on multiple-regression and reliability theory provide useful information on achieving the sustainable design and practice of permeable concrete with the admixtures.

© 2016 Elsevier Ltd. All rights reserved.

1. Introduction

Permeable concrete is an environmentally friendly composite material consisting of cementitious binders, coarse aggregates, water, and other admixtures. Use of permeable concrete is rapidly increasing because of several advantages such as storm-water management, reduced tire-induced pavement noise, and pollutant control [1]. A number of factors influence the performance of permeable concrete installed on site, including the retention of sand-sized particles [2], mixture designs [3], aggregate gradation [4,5], use of recycled aggregate [6], design approaches [7], and service environment such as freeze-thaw [3,8]. Taking into account economic aspects, residual materials such as fly ash or slag are often considered when designing pervious concrete mixtures [9] and their durability has been studied [10]. Infiltration of permeable concrete is considered as the most crucial parameter controlling functionality, including the case with unconventional admixtures [11]. The porosity of permeable concrete and its pore structure have, therefore, extensively been studied previously and their effect was well documented. Typical pore sizes vary between 2 and 8 mm with porosity ranging from 15 to 30% and permeability of 2 to 6 mm/s [12–14]. Haselbach et al. [12] tested permeable concrete to evaluate hydraulic properties: total porosity and saturated hydraulic conductivity. It was suggested that the lower bound of porosity be 15%. A design approach was developed based on the Carman-Kozeny method. Bentz [15]

modeled the porosity of permeable concrete to engage its microstructure with percolation and transport properties. To represent the voids of the concrete, a three-dimensional reconstruction algorithm was employed. The contribution of porosity to durability performance was reported. Neithalath et al. [14] examined a relationship between the porosity and permeability of permeable concrete by characterizing pore volume and sizes. A two-dimensional imaging technique was utilized and the Weibull parameters were fitted to estimate a pore size distribution. Lian et al. [16] developed a theoretical model to study the effect of pore structure on the strength of permeable concrete, including the assessment of existing models. The proposed model well predicted test data as per statistical appraisal.

To comply with recent environmental regulations and recommendations for construction materials such as those of the Environmental Protection Agency (EPA), various alternatives are often used for concrete application. It is recognized that the types of binders influence the performance and service life of constructed multi-material mixtures [17]. Numerous studies have been concerned with the effect of admixtures (e.g., latex, fibers, silica fume, and fine aggregate) on the behavior of permeable concrete [3,13,18] and the effect of synthetic fibers on cementitious composites [19], whereas most of these endeavors are devoted to enhancing mechanical properties and durability (e.g., strength, toughness, and abrasion resistance), rather than characterizing hydraulic performance [2,20]. Another important factor to consider is traffic load that results in raveling of installed permeable concrete and porous-clogging [21], including the influence of instantaneous vehicle loading before mechanical damage is accumulated. Limited research, however, has been conducted on this particular issue from a hydraulic

* Corresponding author.

E-mail addresses: jimmy.kim@ucdenver.edu (Y.J. Kim), adel.gaddafi@ucdenver.edu (A. Gaddafi), yositake@yamaguchi-u.ac.jp (I. Yoshitake).

perspective, while some research results are available about the in-situ behavior of permeable concrete experiencing long-term damage [22, 23]. This paper presents an experimental program assessing the hydraulic performance of various permeable concrete mixtures subjected to instantaneous live load intensity simulating traffic effect (i.e., mechanical load applied within a very short time period), with a focus on admixture-infiltration interaction. Theoretical prediction was carried out to expand laboratory findings, based on multiple regression linked with reliability analysis.

2. Research significance

Although a great deal of research effort has been spent on understanding the behavior of permeable concrete, its hydraulic characteristics when mixed with alternative cost-saving construction materials along with mechanical distress are limitedly studied. There has been no research on multi-material interaction among the constituents of permeable concrete in conjunction with instantaneous traffic load, which is one of the primary sources degrading the in-situ performance of installed permeable concrete, followed by damage accumulation with time. Current knowledge is insufficient to explain technical issues involved in such a service environment where significant live load is applied. The effect of various admixtures in a permeable concrete mixture subjected to instantaneous load intensity needs to be examined to ensure sustainable functionality on site. It is worth noting that the major interest of the present experimental study is in evaluating the performance of such concrete mixtures, rather than in examining the degree of resistance against external attributes based on typical durability test protocols.

3. Experimental program

The performance of various permeable concrete mixtures is examined with an emphasis on hydraulic characteristics in tandem with constituent materials and the intensity of live-load-induced distress. The following summarizes material properties, mixture designs, and test methodologies.

3.1. Materials

Two types of cementitious binders were used: Type III high-early strength portland cement and Class C fly ash [24]. Given the

functionality of fly ash depends upon its chemical composition, a refined material test was conducted. Table 1 summarizes test results, including a comparison with the requirements of ASTM C618 [25] and AASHTO M295 [26]. The coarse aggregates used had a nominal diameter of 9.5 mm. The fibers blended with the binders were two kinds: Ferro-green and Green-net, both of which were commercially available. Ferro-green fibers consist of a mixture of recycled polypropylene and copolymer [27]. Such a combination results in twisted-bundle monofilament that can readily be distributed in a permeable concrete mixture, as shown in Fig. 1(a). The 19 mm long absorption-free fiber includes a specific gravity of 0.91 and is in compliance with ASTM C1116 [28]. Green-net fibers (Fig. 1(b)) are another type of admixture to enhance the behavior of concrete, in particular cracking and toughness, which are made from recycled polypropylene and are non-magnetic and alkali-proof [27]. The fibrillated product has a specific gravity of 0.91 with a length of 19 mm. To replace some portion of aggregates, shredded tire chips were used (Fig. 1(c)). The chips had no steel wires and included a maximum size of 12 mm characterized by ASTM C33 [29]. A specific gravity of 1.1 was measured for these chips according to ASTM C127 [30]. The tire chips were cleansed and dried at room temperature for a minimum of 24 h prior to mixing with other constituents. Fine aggregates were not used in this experimental program.

3.2. Details of mix design

Two permeable concrete categories were designed with and without fly ash, as listed in Table 2. Seven test groups were employed for each one of those categories: RM (regular mix), GN1 and GN2 (1 and 2% replacement of cement with Green-net fibers by mass, respectively), FG1 and FG2 (1 and 2% replacement of cement with Ferro-green fibers by mass, respectively), TC5 and TC10 (5 and 10% replacement of aggregate using tire chips by mass, respectively), and the word 'F' indicated the inclusion of fly ash. Because synthetic fibers are basically two-dimensional, their volumes cannot be accurately controlled and hence a replacement ratio by mass was exploited in this study. The replaced amount of cement for the specimens with fly ash was 20% by mass. It should be noted that such a replacement ratio is less than the permissible limit of 25% specified in ACI-318 [31]. An aggregate-to-cementitious material ratio of 6.5 by mass was maintained, while the water-cementitious material ratio of all the specimens was 0.3 (typically ranging from 0.27 to 0.34 in permeable concrete [32]). All specimens were manually mixed in the laboratory using an electric mixer. Seven concrete cylinders (100 mm in diameter × 200 mm in length) were cast per test group. To evenly distribute the admixtures in the mixed concrete, standard rodding was performed for uniform tamping (i.e., 25 times of rodding in three layers of the concrete). The slump of the concrete mixture was not measured because it would not provide meaningful data for permeable concrete [3]. The demolded cylinders were cured for a week in a moisture-controlled room at a relative humidity of 98% and completely dried for an infiltration test.

3.3. Test procedures

The test protocol used was two-fold: hydraulic properties and mechanical deterioration by instantaneous live load intensity. One-dimensional flow was designed to evaluate the performance of the permeable concrete mixtures, as shown in Fig. 2. To achieve this test condition, all concrete cylinders (Φ100 mm by 200 mm) were wrapped with a membrane layer. Discharge of each specimen was measured seven times with the custom-made infiltrometer until the 400 ml of water completely drained and their average rate was recorded. The use of such a handy infiltrometer was proven to be effective for measuring the hydraulic properties of permeable concrete at a low cost [33]. After measuring the discharge of each specimen,

Table 1
Properties of fly ash tested.

Property		Test result	ASTM C618	AASHTO M295
Chemical tests	Silicon dioxide (SiO ₂), %	30.86	–	–
	Aluminum oxide (Al ₂ O ₃), %	17.13	–	–
	Iron oxide (Fe ₂ O ₃), %	6.17	–	–
	Sum of SiO ₂ , Al ₂ O ₃ , Fe ₂ O ₃ , %	54.16	70.0/50.0 min	70.0/50.0 min
	Calcium oxide (CaO), %	29.53	–	–
	Magnesium oxide (MgO), %	7.84	–	–
	Sulfur trioxide (SO ₃), %	2.70	5.0 max	5.0 max
	Sodium Oxide (Na ₂ O), %	1.93	–	–
	Potassium (K ₂ O), %	0.31	–	–
	Others, %	3.53	–	–
	Physical tests	Moisture content, %	0.00	3.0 max
Loss on ignition, %		0.35	6.0 max	5.0 max
Amount retained on No. 325 sieve, %		14.31	34 max	34 max
Specific gravity		2.77	–	–
Autoclave soundness, %		0.00	0.8 max	0.8 max
SAI, with portland cement at 7 days, % of control		88.0	75 min	75 min
SAI, with portland cement at 7 days, % of control		93.7	75 min	75 min
Water required, % of control	95.0	105 max	105 max	



Fig. 1. Admixtures in permeable concrete: (a) Ferro-green fiber; (b) green-net fiber; (c) shredded tire chip.

Reynolds number (Re) was calculated to characterize the performance of the permeable concrete mixtures tested:

$$Re = \frac{\rho Q d_g}{\mu A} = Q \frac{d_g}{\nu A} \quad (1)$$

where ρ and μ are the density and dynamic viscosity of the water, respectively; Q is the discharge rate (m^3/s); A is the cross sectional area of the specimen perpendicular to flow (m^2); d_g is the representative grain diameter of the permeable concrete (for the present study, $d_g = 9.5$ mm); and ν is the kinetic viscosity of the water ($1.0 \times 10^{-6} \text{ m}^2/\text{s}$ at room temperature). Infiltration was obtained using the discharge Q divided by the cross sectional area A . The hydraulic conductivity (K) of the test specimens was determined using:

$$K = \frac{Q}{iA} \quad (2)$$

where i is the hydraulic gradient. For the present experimental setup, a unit hydraulic gradient may be assumed because of a constant pressure head. Given the large pore size of the permeable concrete, capillary action was negligible.

Selected cylinders were loaded to failure to obtain admixture-dependent compressive strength as per ASTM C39 [34]. Both top and bottom surfaces were capped to prevent local crushing of the specimens. For simulating the damage of permeable concrete caused by traffic load on site, three levels of instantaneous live load intensity were applied using a compression machine: 0%, 50%, and 75% of the capacity of the control RM category (i.e., pre-compression forces of 0 kN, 37 kN, and 55.3 kN, respectively). Previous research reports that such a test scheme was effective to represent in-situ traffic load [35].

Table 2
Test details.

Category	ID	Cement (kg/m^3)	Fly ash (kg/m^3)	Gravel (kg/m^3)	Water (kg/m^3)	Fiber (kg/m^3)	Tire chips (kg/m^3)	
Without fly ash	RM	311	0	2029	93	0	0	
	GN1	308	0	2029	93	3.1	0	
	GN2	305	0	2029	93	6.2	0	
	FG1	308	0	2029	93	3.1	0	
	FG2	305	0	2029	93	6.2	0	
	TC5	311	0	1928	93	0	101	
	TC10	311	0	1827	93	0	202	
	With fly ash	RMF	249	62	2029	93	0	0
		GNF1	246	62	2029	93	2.5	0
		GNF2	244	62	2029	93	5.0	0
FGF1		246	62	2029	93	2.5	0	
FGF2		244	62	1928	93	5.0	0	
TCF5		249	62	1928	93	0	101	
TCF10		249	62	1827	93	0	202	

4. Test results and discussion

Technical results obtained from the mechanical and hydraulic tests are summarized below, including the effect of various admixtures.

4.1. Effect of admixtures on compressive strength

Fig. 3 shows the effect of admixtures on the compressive strength of the permeable concrete. The control RM specimens failed at an average strength of 9.4 MPa. The inclusion of fly ash caused a decrease of 9.6% in strength. This experimental observation is typical for fly ash concrete at early age because all cylinders were tested at 10 days after casting due to use of the high-early strength portland cement (typical permeable concrete is cured for 7 days in practice) and thus the slow pozzolanic reaction of fly ash might not be fully utilized [36]. The fiber admixtures consistently improved the compressive strength of the concrete, as shown in Fig. 3. The average strength of the specimens mixed with Green-net fibers (GN1 and GN2) was 11.7% and 22.3% higher than that of the control RM specimen, respectively. The specimens with fly ash (GNF1 and GNF2) showed a similar trend. The use of Ferro-green fibers was better than that of Green-net fibers: the average strength of the FG categories with and without fly ash was 7.3% and 5.0% greater than that of the GN categories, respectively. This result illustrates that the Ferro-green fibers with the twisted monofilament geometry was more effective than the Green-net fibers having a flat surface in terms of enhancing the interfacial behavior between the cementitious binder and the fibers. The presence of tire chips decreased the compressive strength of the concrete by 9.6% and 21.3% for TC5 and TC10, respectively, in comparison with the strength of the RM specimen. Such an observation is attributed to i) the softening behavior induced by the elastic tire material (i.e., rubberized concrete) and ii) the premature disintegration of the chips from the cementitious binder because of the interfacial stresses developed during the mechanical loading process, accompanying micro-cracking of the binder and slip of the chips [37]. It is worthwhile to note that the effect of air entrapping that can reduce the compressive strength of tire-chip concrete [38,39] is not a significant factor in permeable concrete having large pores. Overall, the inclusion of the fibers exhibited better performance than that of the tire chips from a strength perspective. This conclusion is supported by the mechanical interaction between the cementitious binder and the admixtures. In other words, the fibers continuously transferred mechanical stresses when the binder cracked; however, the chips were not able to do so because of their short geometric configuration.

4.2. Failure mode

Typical failure modes of the permeable concrete specimens loaded in compression are given in Fig. 4. The primary failure of the control RM category was induced by disintegration of the cementitious binder, as shown in Fig. 4(a) and (b). The conventional diagonal failure pattern frequently observed in ordinary concrete cylinders was not noticed due to the contribution of the random pores that caused the localized

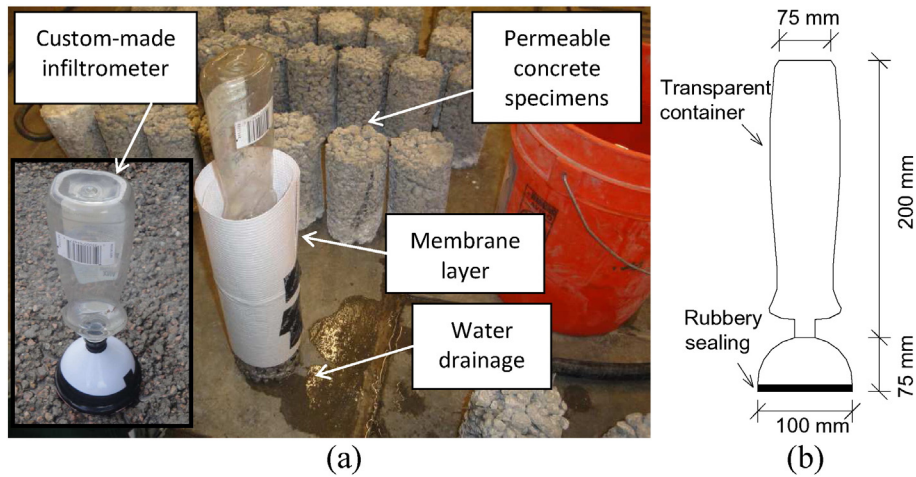


Fig. 2. Experimental details: (a) test in progress; (b) details of infiltrometer.

deformation of the permeable concrete specimens. The fiber-embedded cylinders exhibited a different failure mode relative to the control (Fig. 4(c) and (d)). Fiber-entangling or clustering was not observed in the mixed concrete (Fig. 4(c)), which means that the embedded fibers were evenly distributed in the concrete. The presence of fibers, thus, better distributed internal stresses so that the failure of the specimens was relatively uniform as observed in Fig. 4(d). Other specimens demonstrated similar failure modes (i.e., the tire-chip and fly ash concrete specimens failed in an analogous manner to the RM cylinders, whereas the specimens with Green-net fibers were comparable to the ones with Ferro-green).

4.3. Effect of fibers on infiltration rate

The averaged infiltration rates measured in each test series are provided in Fig. 5(a) with focus on the effect of the embedded fibers. The presence of the fibers, by and large, increased the infiltration rate of the permeable concrete. For example, the specimens mixed with Green-net and Ferro-green fibers demonstrated average increases of 0.8% and 4.5% in infiltration when compared with the control RM, respectively. This observation indicates that i) the embedded fibers created additional voids inside the permeable concrete mix, thereby accelerating the flow of penetrating water and ii) the geometry of the twisted Ferro-green fibers caused more voids than the flat Green-net fibers (i.e., difference in contact surface). The inclusion of fly ash to the control mix without fibers (RMF) caused an increase of 14.1% in infiltration when compared with the RM specimen, as shown in Fig. 5(a). The infiltration of the fly ash concrete, however, tended to decrease with increasing fiber contents: the infiltration rates of GNF and FGF were 14.1% and 16.8% lower than the rate of RMF, on average. There seems to be

some micro-level interaction between the fibers and fly ash in terms of creating voids. Further research is recommended to address this unknown phenomenon.

4.4. Effect of tire chips on infiltration rate

The variation of infiltration with respect to the amount of tire chips is summarized in Fig. 5(b). The average infiltration rates of TC5/TCF5 and TC10/TCF10 were 3.13 mm/s and 2.92 mm/s, respectively. These infiltration rates were 6.0% and 12.3% lower than the average infiltration of RM/RMF. It is, therefore, obvious to report that tire chips have a propensity for clogging permeable concrete and an optimized dosage is recommended when used to improve mechanical properties such as toughness and crack-resistance. The infiltration rate of the tire-chip specimens was lower than that of those with the fibers (Fig. 5(b)). The average infiltration of the TC/TCF categories showed decreases of 3.2% and 2.6% in comparison with that of the GN/GNF and FG/FGF counterparts, respectively. This observation can be explained by the fact that the aggregate-like tire chips blocked more pores of the permeable concrete than the relatively small fibers. The effect of fly ash on the tire-chip concrete was found to be similar to that of the fiber-embedded ones discussed earlier.

4.5. Effect of instantaneous live load intensity on hydraulic properties

Fig. 6 compares the infiltration rate of the permeable concrete subjected to various levels of instantaneous live load intensity. The cylinders exposed to these traffic load effects exhibited a significant reduction in infiltration. The overall average decrease of infiltration was 51.3% and 63.1% for the cylinders subjected to 50% and 75% of

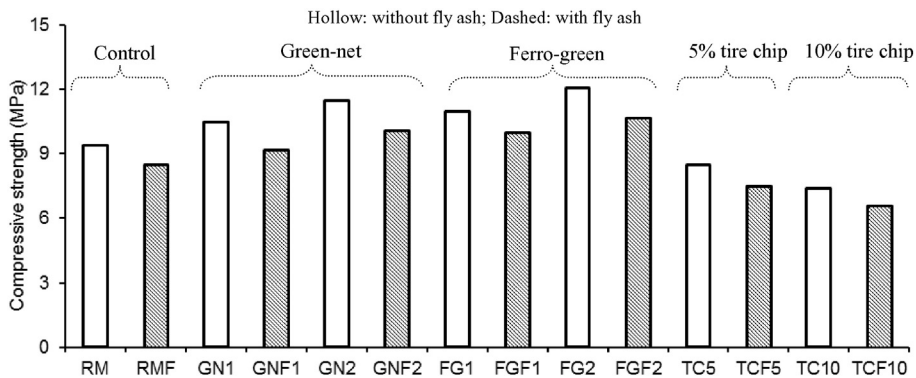


Fig. 3. Effect of admixtures on compressive strength.

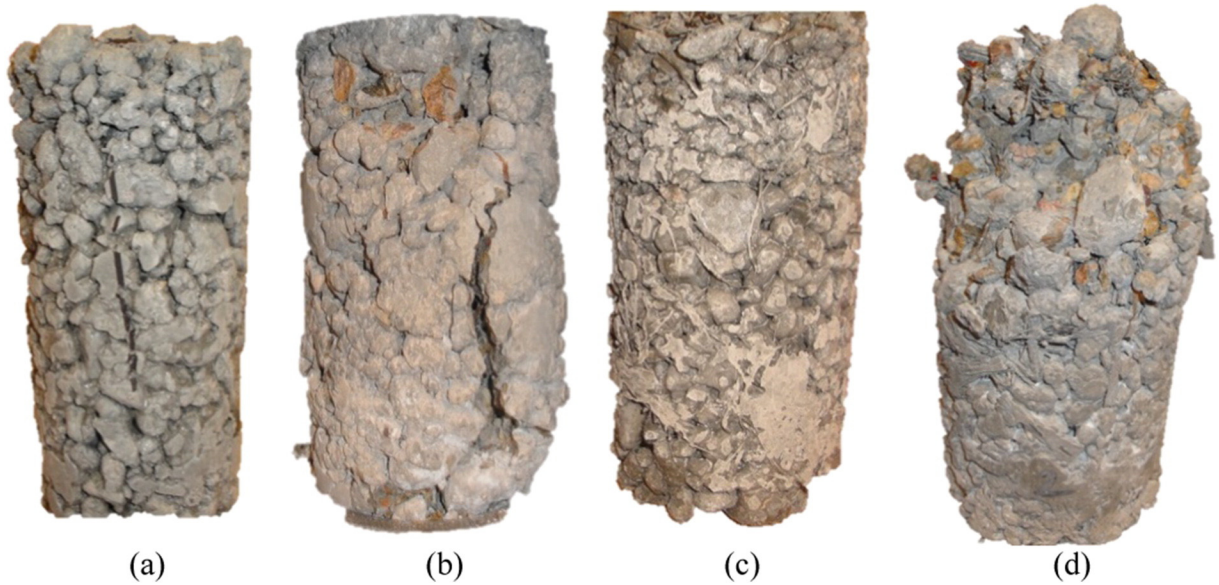


Fig. 4. Failure mode: (a) RM specimen before loading; (b) RM specimen after loading; (c) FG2 specimen before loading; (d) FG2 specimen after loading.

instantaneous intensity (designated 50% load and 75% load in Fig. 6), respectively, relative to the infiltration of the specimens without such a live load effect (0% load). The contribution of the instantaneous live load to a reduction in infiltration was reliant upon admixture types: the specimens with tire chips were more susceptible to the live load intensity than those with fibers, as shown in Fig. 6. For example, the average reduction of infiltration was 11.9% and 7.9% for the specimens having the tire chips (TC) and fibers (GN and FG), respectively, in comparison with the control (RM) when the live load intensity increased from 0% to 75%. These reduction rates became more pronounced with the mix of fly ash, leading to 15.2% and 10.7% for the tire chip and the fiber categories, respectively. Such observations illustrate i) the cementitious binders were damaged due to the instantaneous load and their debris clogged micro-pores of the permeable concrete, ii) interfacial damage between the binder and tire chips was more vulnerable to the external load than that of the fibers, and iii) the damage of the fly-ash-hybrid binder was more critical than that of the homogeneous portland cement binder.

Other hydraulic characteristics of the permeable concrete tested are summarized in Table 3. The regional failure of the cementitious binder due to the live load effect significantly reduced the Reynolds number (i.e., increased clogging). The Reynolds number of the specimens without fly ash (RM, GN, FG, and TC categories) subjected to 0%, 50%, and 75% load were 30.7, 15.3, and 11.5, on average, and similar values were obtained for those with fly ash (30.8, 14.1, and 10.8, respectively).

These Reynolds numbers greater than 10 imply that the flow of water penetrating the permeable concrete was a kind of turbulence flow. Physical interpretation of this observation is that a stochastic flow has occurred and hence inertia effect tended to dominate the flow over viscous effect, while the water passed through the concrete specimens. The hydraulic conductivity of the tested permeable concrete (K) was also substantially influenced by the instantaneous live load intensity, as shown in Table 3. The control RM specimen exhibited decreases of 45.6% and 61.2% in hydraulic conductivity when the live load effect increased from 0% to 50% and to 75%, respectively. The specimens mixed with the fibers and tire chips demonstrated higher decreases than the RM category; for instance, the TC specimens showed reductions of 52.7% and 63.3%, on average, with increases in the instantaneous load from 0% to 50% and to 75%, respectively. When the permeable concrete was mixed with fly ash, the influence of the live load was more noticeable, as shown in Fig. 7 where normalized comparisons are given (i.e., a ratio of the hydraulic conductivity of a certain load intensity to that of 0% load). The reduction of hydraulic conductivity of the RMF category was 18.8% higher than that of the RM counterpart with an increase in live load effect from 0% to 50%. Other specimens with the admixtures showed a similar trend. These observations imply that significant traffic load on site results in clogging of the permeable concrete, thereby reducing hydraulic conductivity, and use of fly ash needs additional considerations when designing permeable concrete in such a service environment. It is also worthwhile to note that, from a practice point

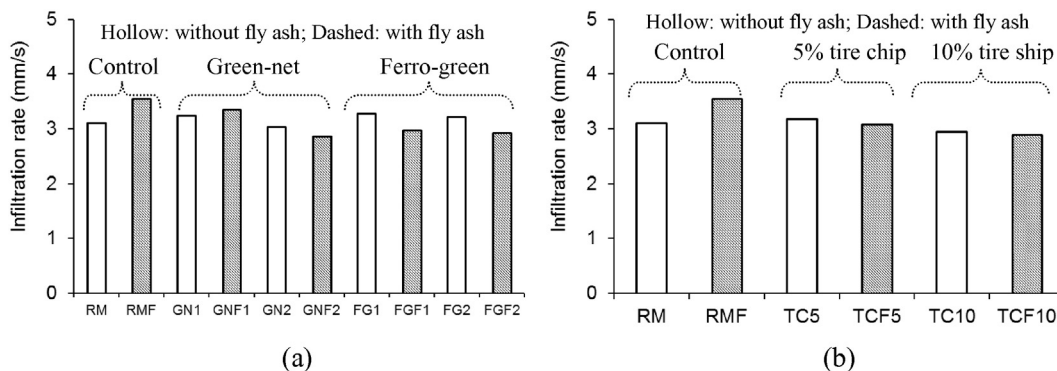


Fig. 5. Variation of infiltration rate: (a) effect of embedded fibers; (b) effect of tire chips.

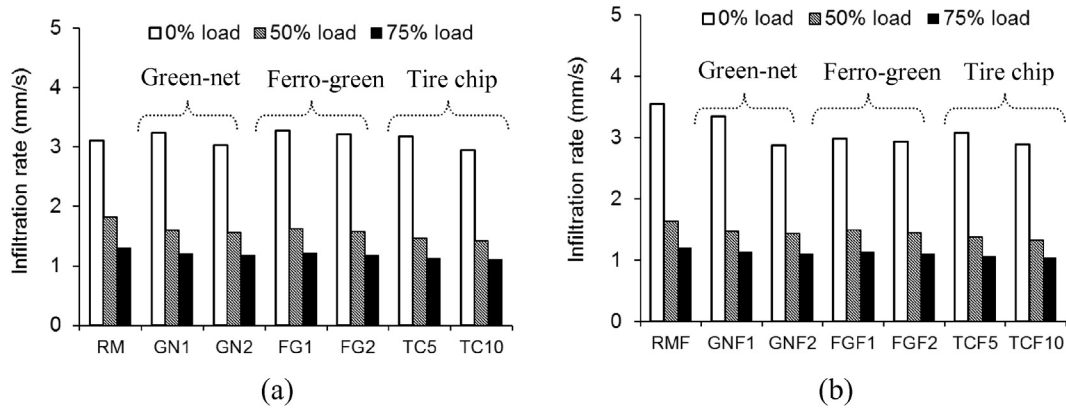


Fig. 6. Effect of instantaneous live load intensity on infiltration rate: (a) specimens without fly ash; (b) specimens with fly ash.

of view, the effect of clogging in permeable concrete needs to be linked with the type of base course (e.g., clean sand or other soils).

5. Predictive model

A descriptive statistics approach is employed to represent the performance of the permeable concrete mixtures having various admixtures subjected to instantaneous live load. Given below are a summary of the model development and a parametric study.

5.1. Regression for hydraulic properties of permeable concrete

The hydraulic properties of the tested permeable concrete were modeled by multiple regression [40], including all the variables listed in Table 2. The infiltration rate of the specimens was fitted using the experimental data, as shown in Eq. (3) (the coefficient of determination was $R^2 = 0.9666$):

$$Inf_p = 0.089573C + 0.088128F + 0.00034G + 0.050315F_b - 0.00135T_r - 0.02729L - 25.2605 \quad (3)$$

where Inf_p is the predicted infiltration rate (mm/s); $C, F, G, F_b,$ and T_r are the amounts of portland cement, fly ash, gravel, fibers (Ferro-green and Green-net concurrently), and tire chips in kg/m^3 ; and L is the live load intensity in percent. The water content was constant in this experimental program and thus its contribution to Eq. (3) was none from a

regression view point. The predicted hydraulic conductivity of the permeable concrete (K_p) was also provided:

$$K_p = 0.175279C + 0.174704F + 0.000675G + 0.138756F_b - 0.00054T_r - 0.02846L - 52.542. \quad (4)$$

Another version of regression equations to predict the infiltration rate and hydraulic conductivity of the concrete is proposed with an emphasis on the effect of instantaneous live load:

$$Inf_p(L) = ae^{bL} \quad (5)$$

$$K_p(L) = ae^{bL} \quad (6)$$

where $Inf_p(L)$ and $K_p(L)$ are the predicted infiltration rate and hydraulic conductivity with respect to the level of instantaneous live load; and a and b are empirical constants. Table 4 summarizes the constants obtained from experimental curve-fitting as well as the coefficient of determination (R^2). The constants listed in Table 4 are based on metric units, while the predicted hydraulic properties can readily be converted to those in the US customary units. As shown in Fig. 8 and Table 4, the degree of regression was satisfactory. It should be noted that Eqs. (3) and (4) are used for examining the effect of each constituent on the performance of the permeable concrete, while Eqs. (5) and (6) are relevant to concentrating on the effect of live load that is a critical parameter influencing the hydraulic properties of the concrete.

Table 3 Effect of instantaneous live load intensity measured from the test.

Category	ID	0% load			50% load			75% load		
		Inf (mm/s)	Re	K (mm/s)	Inf (mm/s)	Re	K (mm/s)	Inf (mm/s)	Re	K (mm/s)
Without fly ash	RM	3.33	32.3	3.40	1.82	17.6	1.85	1.30	12.6	1.32
	GN1	3.24	31.4	3.31	1.60	15.5	1.63	1.20	11.7	1.23
	GN2	3.03	29.3	3.08	1.54	14.9	1.57	1.18	11.4	1.20
	FG1	3.27	31.7	3.34	1.62	15.7	1.65	1.22	11.8	1.24
	FG2	3.22	31.2	3.28	1.57	15.2	1.60	1.18	11.5	1.21
	TC5	3.18	30.8	3.24	1.47	14.3	1.50	1.14	11.0	1.16
	TC10	2.95	28.5	3.00	1.42	13.8	1.45	1.11	10.7	1.13
With fly ash	RMF	3.55	34.4	3.62	1.63	15.8	1.66	1.20	11.6	1.22
	GNF1	3.35	32.4	3.42	1.47	14.2	1.50	1.13	11.0	1.15
	GNF2	2.87	27.8	2.93	1.43	13.8	1.46	1.10	10.7	1.13
	FGF1	2.98	28.1	2.96	1.49	14.4	1.52	1.14	11.0	1.16
	FGF2	2.93	28.5	3.00	1.45	14.0	1.47	1.11	10.7	1.13
	TCF5	3.08	29.8	3.14	1.37	13.3	1.40	1.06	10.3	1.08
	TCF10	2.89	34.5	3.63	1.33	12.9	1.35	1.04	10.1	1.06

Inf = infiltration rate; Re = Reynolds number; K = hydraulic conductivity.

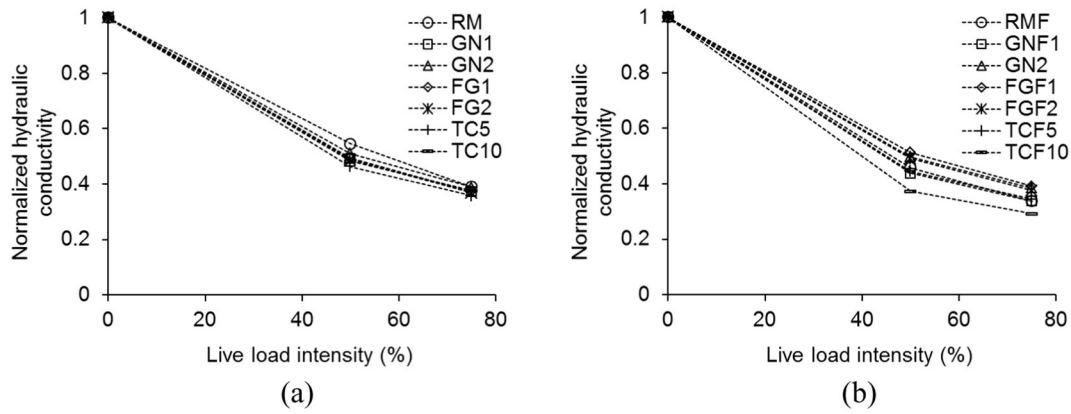


Fig. 7. Normalized comparison of hydraulic conductivity depending upon instantaneous live load intensity: (a) specimens without fly ash; (b) specimens with fly ash.

5.2. Parametric investigation

Fig. 9 shows the effect of various admixtures on the infiltration of the permeable concrete, depending upon the level of instantaneous live load intensity and a combination of constituent materials. To carry out these parametric investigations using Eq. (3), the following base-line properties were employed in compliance with the mixture designs described in Table 2: the amount of fly ash or fibers (kg/m^3) equals $311 \text{ kg}/\text{m}^3$ minus the amount of portland cement (kg/m^3) and the amount of tire chips (kg/m^3) is equal to $2029 \text{ kg}/\text{m}^3$ minus the amount of gravel (kg/m^3). Extrapolation of Eq. (3) was not allowed (i.e., the quantities of these constituents were within the variation ranges shown in Table 2). It is important to note that the present parametric study was intended to examine the tendency of specific constituent materials' contribution to the hydraulic property of the permeable concrete, rather than measuring their influence as reported in the experimental program. The existence of fly ash resulted in a negligible

variation of infiltration (Fig. 9(a)), however the effect of tire chips was noticeable with a maximum variation of 37.8% (Fig. 9(b)). The inclusion of the fibers considerably decreased the infiltration of the permeable concrete as low as 45.9% (Fig. 9(c)). This result illustrates the optimum dosage of fibers benefits the performance of permeable concrete, as discussed in Figs. 3 and 5, whereas excessive amounts of fibers will be detrimental. It is worth noting that the minor discrepancy between Figs. 3 and 9(c) in terms of the fiber effect is attributed to the nature of the regression model. The contribution of the instantaneous live load was substantial to all cases. The response of hydraulic conductivity (K) in conjunction with these parameters was similar to that of the infiltration discussed above (not shown here for brevity).

5.3. Performance assessment

The level of instantaneous live load intensity was the most critical parameter affecting the performance of permeable concrete, as

Table 4
Constants for simplified regression equation.

Category	ID	Parameter	Mean			Standard deviation		
			a	b	R^2	a	b	R^2
Without fly ash	RM	Hydraulic conductivity	3.4117	-0.013	0.999	0.3406	-0.032	0.992
		Infiltration rate	3.3478	-0.013	0.999	0.3342	-0.032	0.992
	GN1	Hydraulic conductivity	3.2715	-0.013	0.997	0.1179	-0.019	0.980
		Infiltration rate	3.2101	-0.013	0.997	0.1157	-0.019	0.980
	GN2	Hydraulic conductivity	3.0556	-0.013	0.997	0.1827	-0.027	0.999
		Infiltration rate	2.9983	-0.013	0.997	0.1793	-0.027	0.999
	FG1	Hydraulic conductivity	3.3054	-0.013	0.997	0.0964	-0.017	0.919
		Infiltration rate	3.2434	-0.013	0.998	0.0946	-0.017	0.919
	FG2	Hydraulic conductivity	3.2496	-0.013	0.997	0.3928	-0.045	0.879
		Infiltration rate	3.1887	-0.013	0.997	0.3854	-0.045	0.879
TC5	Hydraulic conductivity	3.1823	-0.014	0.992	0.4284	-0.047	0.990	
	Infiltration rate	3.1226	-0.014	0.992	0.4203	-0.047	0.991	
TC10	Hydraulic conductivity	2.9545	-0.013	0.992	0.3256	-0.059	0.997	
	Infiltration rate	2.8991	-0.013	0.993	0.3194	-0.059	0.998	
With fly ash	RMF	Hydraulic conductivity	3.5747	-0.015	0.996	0.5585	-0.046	0.877
		Infiltration rate	3.5077	-0.015	0.997	0.5480	-0.046	0.878
	GNF1	Hydraulic conductivity	3.3429	-0.015	0.990	0.4787	-0.053	0.960
		Infiltration rate	3.2802	-0.015	0.990	0.4697	-0.053	0.960
	GNF2	Hydraulic conductivity	2.8880	-0.013	0.995	0.0867	-0.020	0.992
		Infiltration rate	2.8339	-0.013	0.995	0.0851	-0.020	0.992
	FGF1	Hydraulic conductivity	2.9348	-0.013	0.997	0.1963	-0.033	0.920
		Infiltration rate	2.9445	-0.013	0.997	0.1725	-0.031	0.922
	FGF2	Hydraulic conductivity	2.9650	-0.013	0.995	0.1294	-0.027	0.922
		Infiltration rate	2.8923	-0.013	0.996	0.1101	-0.024	0.925
	TCF5	Hydraulic conductivity	3.0749	-0.015	0.989	0.2066	-0.034	0.996
		Infiltration rate	3.0172	-0.015	0.990	0.2027	-0.034	0.996
	TCF10	Hydraulic conductivity	3.5052	-0.017	0.979	0.3982	-0.059	0.985
		Infiltration rate	2.8356	-0.014	0.990	0.1841	-0.048	0.947

a and b = empirical constants; R^2 = coefficient of determination.

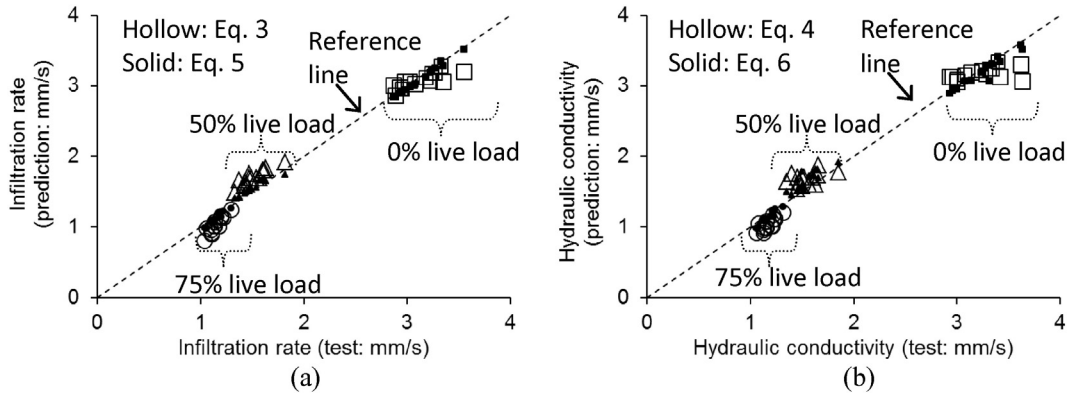


Fig. 8. Assessment of proposed equations: (a) infiltration rate; (b) hydraulic conductivity.

discussed earlier. Provided that the presence of traffic load on site is stochastic, deterministic approaches have fundamental limitations in assessing the hydraulic characteristics of such a concrete. Progressive degradation of installed permeable concrete with an increasing live load effect was thus probabilistically examined using the first-order reliability method. The following summarizes the reliability formulation used for the present study, while further details are available elsewhere [41]. The performance function of permeable concrete is given in Eq. (7):

$$g(Infp(L), Inf_{th}) = Inf_p(L) - Inf_{th} \tag{7}$$

where Inf_{th} is the threshold infiltration limit of the permeable concrete depending upon a region where a storm water event takes place. Performance degradation is expected when Eq. (7) generates a negative value and corresponding probability is determined using Eq. (8):

$$Pr(L) = Pr(Infp(L) \leq Inf_{th}) \tag{8}$$

where $Pr(L)$ is the probability of performance degradation of the permeable concrete subjected to an arbitrary level of traffic load intensity L . The infiltration functions, $Inf_p(L)$ and Inf_{th} , are transformed to standard normal for facilitating probabilistic investigations, including the standard normal random variables U . The norm of vector $\nabla g(U_0(L))$ is then obtained using Eq. (9):

$$\|\nabla g(U_0(L))\| = \sqrt{\sigma_{Inf_p}^2(L) + \sigma_{Inf_{th}}^2} \tag{9}$$

but

$$g(U_0(L)) = Inf_p(L) - Inf_{th}(L) \tag{10}$$

where $\nabla g(U_0(L))$ is the gradient of the initial random variable U_0 ; and $\sigma_{Inf_p}(L)$ and $\sigma_{Inf_{th}}$ are the standard deviations of the live-load-

dependent infiltration and the threshold limit, respectively. After constructing a ratio of the gradient of the performance function to its norm α_0 and acquiring the norm of the initial random variable β_0 [41], the reliability index β is expressed as the most probable point within the probabilistic domain U^* :

$$\beta = \|U^*\| \text{ in which } U^* = -\alpha_0[\beta_0 + \nabla g(U_0)/\|\nabla g(U_0)\|] \tag{11}$$

The probability of performance degradation is estimated:

$$Pr = \Phi(\beta) \text{ or } \Phi(-\beta) \tag{12}$$

where $\Phi(\beta)$ or $\Phi(-\beta)$ is the cumulative density function of the standard normal distribution. To implement the reliability approach described above, the infiltration rate functions of the permeable concrete studied (Eq. (5) and Table 4) were utilized. It should be noted that the focus of the present probabilistic investigation was on the effect of live load due to its technical significance and thus Eq. (5) was more relevant to use than Eq. (3). For a demonstration purpose, the threshold infiltration limit was taken from the suggestion of the Minnesota Department of Transportation [33], leading to an infiltration of 2.54 mm/s for the current test setup and corresponding coefficient of variation of 0.56 (based on the measured data in MnDOT [33]).

Fig. 10 shows the predicted response of the permeable concrete mixes with respect to the level of live load intensity. Performance degradation in terms of infiltration gradually increased up to a live load intensity of 50% beyond which all specimens exceeded a probability of degradation of 0.8 (i.e., the infiltration rate of these concrete mixes was sufficiently lower than the threshold limit). The inclusion of various admixtures tended to accelerate the degradation of the infiltration rate, as shown in Fig. 10(a) and (b). This fact implies that multi-material interaction, when live load is present, can cause deterioration of the cementitious binder and produce residual debris that clogs the pores of the permeable concrete. The categories mixed with fly ash demonstrated larger variation ranges in degradation probability (Fig. 10(b))

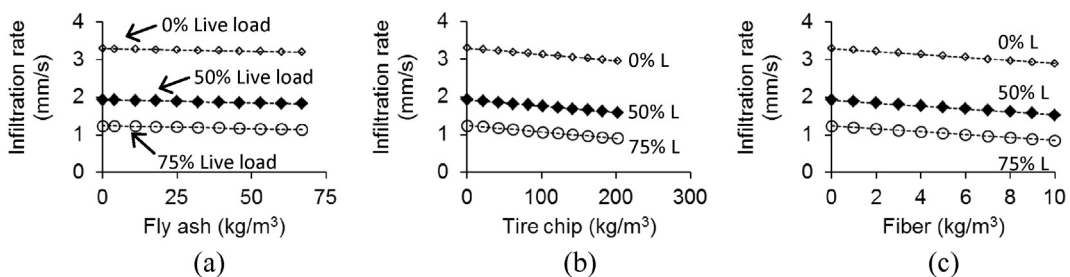


Fig. 9. Effect of admixtures in conjunction with instantaneous live load intensity (C: portland cement, F: fly ash, F_b : fiber, G: aggregate, and L: live load effect): (a) fly ash (constituents: C + F + G + L); (b) tire chip (constituents: C + G + T_r + L); (c) fiber (constituents: C + G + F_b + L).

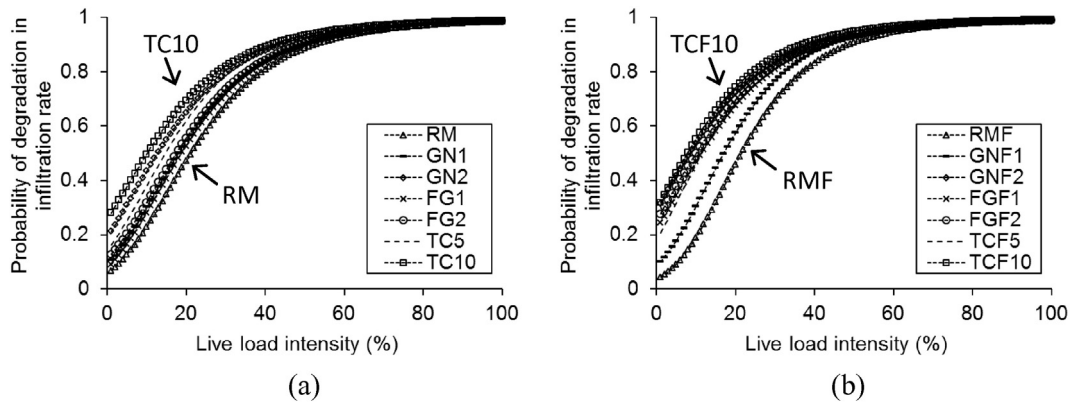


Fig. 10. Predicted degradation of infiltration due to live load effect: (a) permeable concrete without fly ash; (b) permeable concrete with fly ash.

compared with those without fly ash (Fig. 10(a)), confirming the multi-material interaction mechanism mentioned above.

6. Summary and conclusions

This paper has dealt with various permeable concrete mixtures having alternative construction materials subjected to instantaneous live load intensity ranging from 0% to 75% of the control strength. Specimens were classified into two groups depending upon the presence of fly ash and each group had seven cylinders mixed with non-metallic fibers and tire chips. Experimental results characterized the performance of these permeable concrete mixtures in terms of load-bearing capacity and hydraulic properties such as infiltration, Reynolds numbers, and hydraulic conductivity. A predictive approach was present based on multiple-regression and reliability theory. The following conclusions are drawn:

- The presence of fly ash decreased the compressive strength of the permeable concrete relative to the test category without fly ash. The specimens mixed with the fibers exhibited improved strength and their geometric configuration affected the extent of strength increase. The specimens including tire chips showed a decreased strength because of their elastic softening nature and premature disintegration from the cementitious binders.
- The failure of the control and tire-chip concrete was due to the localized disintegration of the cementitious binder in conjunction with the randomly distributed pores. The test category mixed with the fibers demonstrated relatively even failure without noticeable fiber-entangling.
- The inclusion of the fibers enhanced the infiltration rate of the permeable concrete and the twisted fibers created more pores than the flat ones. The effect of fly ash on infiltration was dependent upon the interaction with other constituents. Tire chips tended to clog pores and decreased infiltration.
- Instantaneous live load intensity was a significant parameter degrading the hydraulic performance of the permeable concrete. Some correlations between the live load effect and the admixtures were observed such that the tire chips were more vulnerable than the fibers in terms of reducing infiltration capacity, however fly ash accelerated performance degradation with increased clogging.
- The comparative parametric investigation implied that the fibers were a critical parameter that could clog the pores of the permeable concrete if used excessively, alternative admixtures replacing conventional constituents of permeable concrete (i.e., fly ash and tire chips) to enhance mechanical properties may be used with reasonable amounts without concerns of degrading hydraulic properties, and excessive traffic load is detrimental to the performance of permeable concrete.

Acknowledgments

The authors gratefully acknowledge support from Holcim Inc. and FORTA Corporation. The scholarship program provided by the Libyan Government to the second author is appreciated. The findings discussed in this paper represent the opinion of the writers and do not necessarily reflect the opinion of others.

References

- [1] ACI, Pervious Concrete (ACI522R-06), American Concrete Institute Committee 522, 2006 (Farmington Hills, MI).
- [2] J.P. Coughlin, C.D. Campbell, D.C. Mays, Infiltration and clogging by sand and clay in a pervious concrete pavement system, *J. Hydrol. Eng.* 17 (1) (2012) 68–73.
- [3] J.T. Keven, V.R. Schaefer, K. Wang, M.T. Suleiman, Pervious concrete mixture proportions for improved free-thaw durability, *J. ASTM Int.* 5 (2) (2008) (Paper ID JA1101320).
- [4] K.C. Mahboub, J. Canler, R. Rathbone, T. Robl, B. Davis, Pervious concrete: compaction and aggregate gradation, *ACI Mater. J.* 106 (6) (2009) 523–528.
- [5] A.I. Neptune, B.J. Putman, Effect of aggregate size and gradation on pervious concrete mixtures, *ACI Mater. J.* 107 (6) (2010) 625–631.
- [6] E. Guneyisi, M. Gesoglu, Q. Kareem, S. Ipek, Effect of different substitution of natural aggregate by recycled aggregate on performance characteristics, *Mater. Struct.* 49 (2016) 521–536.
- [7] T.C. Fu, R. Huang, W.C. Yeih, J.J. Chang, P.C. Lee, Study of the pervious concrete properties using the experimental design method, *Adv. Mater. Res.* 1089 (2015) 253–264.
- [8] Z. Yang, Freezing-and thawing durability of pervious concrete under simulated field conditions, *ACI Mater. J.* 108 (2) (2011) 187–195.
- [9] J.J. Chang, W. Yeih, T.J. Chung, R. Huang, Properties of pervious concrete made with electric arc furnace slag and alkali-active slag cement, *Constr. Build. Mater.* 109 (2016) 34–40.
- [10] I. Anderson, M.M. Dewoolkar, Laboratory freezing-and-thawing durability of fly ash pervious concrete in a simulated field environment, *ACI Mater. J.* 112 (5) (2015) 603–611.
- [11] L. Gola, V. Vaclavik, J. Valicek, M. Harnicarova, M. Kusnerova, T. Dvorsky, Drainage concrete based on cement composite and industrial waste, *Mech. Mater. Eng. Mod. Struct. Component Des.* 70 (2015) 155–165.
- [12] L.M. Haselbach, S. Valavala, F. Montes, Permeability predictions for sand-clogged Portland cement pervious concrete pavement systems, *J. Environ. Manag.* 81 (1) (2006) 42–49.
- [13] B. Huang, H. Wu, X. Shu, E.G. Burdette, Laboratory evaluation of permeability and strength of polymer-modified pervious concrete, *Constr. Build. Mater.* 24 (2010) 818–823.
- [14] N. Neithalath, M.S. Sumanasooriya, D. Omkar, Characterizing pore volume, sizes, and connectivity in pervious concretes for permeability prediction, *Mater. Charact.* 61 (2010) 802–813.
- [15] D.P. Bentz, Virtual pervious concrete: microstructure, percolation, and permeability, *ACI Mater. J.* 105 (3) (2008) 297–301.
- [16] C. Lian, Y. Zhuge, S. Beecham, The relationship between porosity and strength for porous concrete, *Constr. Build. Mater.* 25 (2011) 4294–4298.
- [17] A. Jamshidi, M.O. Hamzah, K. Kurumisawa, T. Nawa, B. Samali, Evaluation of sustainable technologies that upgrade the binder performance grade in asphalt pavement construction, *Mater. Des.* 95 (2016) 9–20.
- [18] J. Yang, G. Jiang, Experimental study on properties of pervious concrete pavement materials, *Cem. Concr. Res.* 33 (2003) 381–386.
- [19] S.H. Said, H.A. Razak, The effect of synthetic polyethylene fiber on the strain hardening behavior of engineered cementitious composite, *Mater. Des.* 86 (2015) 447–457.
- [20] K.G. Modeste, L.C. Falls, P.Y. Park, Performance of permeable pavements under low volume traffic loads, 94th Annual Meeting of the Transportation Research Board, Washington, D.C., 2015.

- [21] A.S. Hager, Sustainable Design of Pervious Concrete Pavements, 2009 (PhD Dissertation, University of Colorado Denver, Denver, CO).
- [22] M. Kayhanian, D. Anderson, J.T. Harvey, D. Jones, B. Munhunthan, Permeability measurement and scan imaging to assess clogging of pervious concrete pavements in parking lots, *J. Environ. Manag.* 95 (2012) 114–123.
- [23] K. Kumar, J. Kozak, L. Hundal, A. Cox, H. Zhang, T. Granato, In-situ infiltration performance of different permeable pavements in an employ used parking lot - a four-year study, *J. Environ. Manag.* 167 (2016) 8–14.
- [24] A.M. Neville, Properties of Concrete, 4th edition Pearson, Essex, UK, 1995.
- [25] ASTM, Standard Specifications for Coal Fly Ash and Raw or Calcined Natural Pozzolan for Use in Concrete (ASTM C618), American Society for Testing and Materials, West Conshohocken, PA, 2012.
- [26] AASHTO, Standard Specifications for Coal Fly Ash and Raw or Calcined Natural Pozzolan for Use in Concrete, American Association of State Highway and Transportation Officials, Washington, D.C., 2011.
- [27] FORTA, Manufacturer Fact-data, FORTA Corporation, Grove City, PA, 2013.
- [28] ASTM, Standard Specifications for Fiber-reinforced Concrete (ASTM C1116), American Society for Testing and Materials, West Conshohocken, PA, 2010.
- [29] ASTM, Standard Specifications for Concrete Aggregates (ASTM C33), American Society for Testing and Materials, West Conshohocken, PA, 2013.
- [30] ASTM, Standard Test Method for Density, Relative Density (Specific Gravity), and Absorption of Coarse Aggregate (ASTM C127), American Society for Testing and Materials, West Conshohocken, PA, 2012.
- [31] ACI, Building Code Requirements for Structural Concrete and Commentary (ACI318-14), 2014 (Farmington Hills, MI).
- [32] T. Tennis, M. Leming, D. Akers, Pervious Concrete Pavements, Portland Cement Association, Skokie, IL, 2004.
- [33] MnDOT, MnROAD Cell 64 Pervious Concrete: Third Year Performance Report, Minnesota Department of Transportation, St. Paul, MN, 2009.
- [34] ASTM, Standard Test Method for Compressive Strength of Cylindrical Concrete Specimens (ASTM C39), American Society for Testing and Materials, West Conshohocken, PA, 2012.
- [35] M. Hossain, Y.J. Kim, Effects of instantaneous live load on the performance of constructed concrete members in cold regions, *J. Perform. Constr. Facil.* 26 (4) (2012) 478–488.
- [36] C. Lima, A. Caggiano, C. Faella, E. Martinelli, M. Pepe, R. Realfonzo, Physical properties and mechanical behavior of concrete made with recycled aggregates and fly ash, *Constr. Build. Mater.* 47 (2013) 547–559.
- [37] G. Li, M.A. Stunlefield, G. Garrick, J. Eggers, C. Abadie, B. Huang, Development of Waste Tire Modified Concrete, 34, 2283–2289, 2004.
- [38] Z.K. Khatib, F.M. Bayomy, Rubberized portland cement concrete, *J. Mater. Civ. Eng.* 11 (3) (1999) 206–213.
- [39] A. Bennazzouk, O. Douzane, T. Langlet, K. Mezreb, J.M. Roucoult, M. Queneudec, Physico-mechanical properties and water absorption of cement composite containing shredded rubber wastes, *Cem. Concr. Compos.* 29 (2007) 732–740.
- [40] D.C. Montgomery, G.C. Runger, Applied Statistics and Probability for Engineers, John Wiley & Sons, New York, NY, 2003.
- [41] Y.J. Kim, M. Hossain, J. Zhang, A probabilistic investigation into deterioration of CFRP-concrete interface in aggressive environments, *Constr. Build. Mater.* 41 (2013) 49–59.